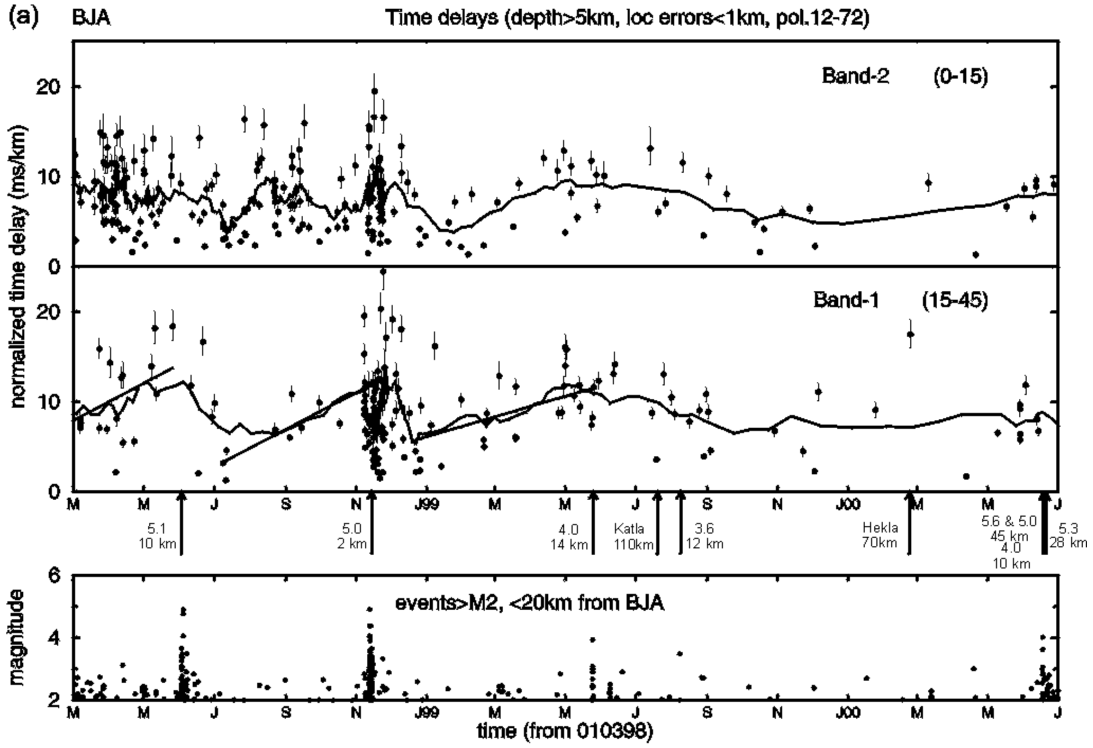
(a)
BJA
Time delays (depth>5km, loc errors<1km, pol.12-72)
normalized time delay (ms/km)
Band-2 (0-15)
Band-1 (15-45)
M M J S N J99 M M J S N J00 M M J
5.1
10 km
5.0
2 km
4.0
14 km
Katla
110km
3.6
12 km
Hekla
70km
5.6 & 5.0
45 km
4.0
10 km
5.3
28 km
magnitude
events>M2, <20km from BJA
time (from 010398)

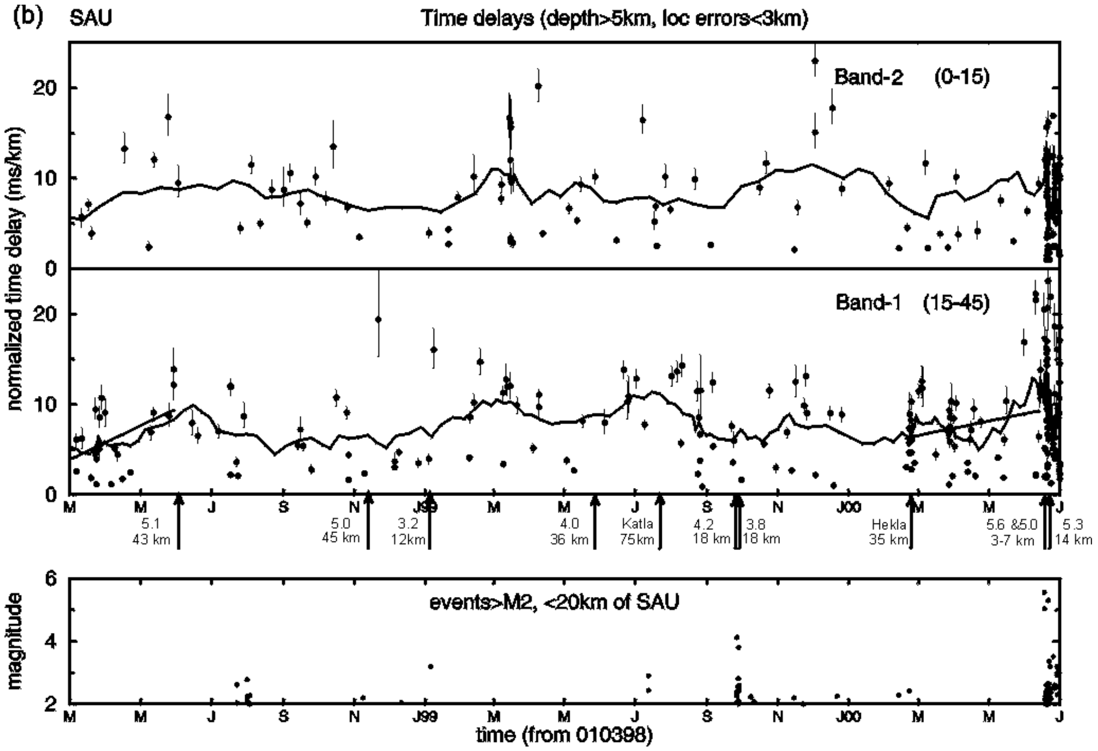
(b)
SAU
Time delays (depth>5km, loc errors<3km)
normalized time delay (ms/km)
Band-2 (0-15)
Band-1 (15-45)
M M J S N J99 M M J S N J00 M M J
5.1
43 km
5.0
45 km
3.2
12km
4.0
36 km
Katla
75km
4.2
18 km
3.8
18 km
Hekla
35 km
5.6 &5.0
3-7 km
5.3
14 km
magnitude
events>M2, <20km of SAU
time (from 010398)

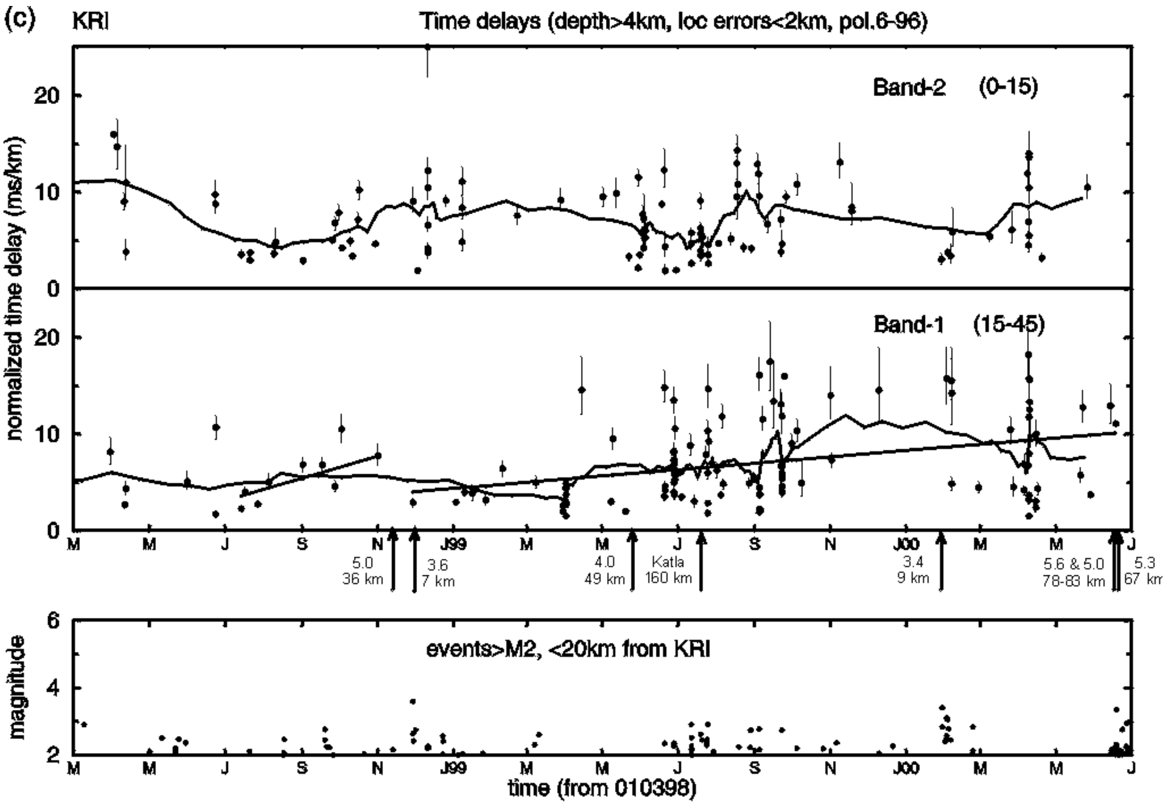

Figure 10. *Shear-wave splitting at BJA (a), SAU (b) and KRI (c) from March 1, 1998 to June 31, 2000. The upper and middle cartoons show variaton of normalized time-delays with time, for ray paths in bands with incidence* $0°$ *to* $15°$ *to the crack face (Band-2) and with incidence* $15°$ *to* $45°$ *to the crack face (Band-1). Band-2 is sensitive to crack density whereas Band-1 is sensitive to aspect ratio. There are nine-point moving averages through the time-delays. Lines are least square fits to data before a major earthquake. The lower cartoons show the magnitudes of* $M \geq 2$ *earthquakes within 20 km of each station.*

stress-forecast within a comparative narrow time-magnitude window.

During June 2000, three large earthquakes occurred near SAU. Although time-delays in Band-1 seemed to increase about four months before the first event of June 17, these earthquakes were not stress-forecast. The main reason was that before the swarm of activity in February associated with Hekla (Figure 10b), there was a period of about four weeks without any suitable shear-wave source earthquakes, and consequently no reliable time-delay measurements and reliable slopes and durations of the increase could not be identified.

October 27	UEDIN.DGG emails IMOR.DG reporting shear-wave time-delays in Band-1 increasing from July at stations BJA and KRI and suggests: *". . . there was an 80% chance of something significant happening somewhere between BJA and KRI within three months."**
October 28	UEDIN.DGG faxes data for BJA and KRI to IMOR.DG. IMOR.DG suggests M=5.1 earthquake near BJA in June 1998 may be linked to current increase in time-delays.
October 29	UEDIN.DGG updates current interpretation and suggests: *"Shear-wave splitting at both BJA and KRI indicate something is going to happen soon, probably within a month . . ."**
October 30	IMOR.DG sends notice to National Civil Defence (NCD) in Reykjavík suggesting a meeting.
October 31 -November 4	Faxes and emails updating information. UEDIN.DGG refines data and interpretation. IMOR.DG creates local geophysical and geological investigations.
November 5	IMOR.DG presents stress-forecast and other data from surrounding area to scientific advisors of NCD, who conclude no further action was required of them.
November 6-9	Exchange of various faxes and emails updating information and interpretation.
November 10	UEDIN.DGG concludes: *". . . the last plot . . . is already very close to 10 ms/km. This means that an event could occur any time between now (M$\geq$5) and end of February (M$\geq$6) ."**
November 11	UEDIN.DGG faxes updated data for KRI and BJA, with SAU now also suggesting increasing time-delays from September.
November 13	IMOR.DG reports: *". . . here was a magnitude 5 earthquake just near to BJA (preliminary epicenter 2 km west of BJA) this morning at 10:38 GMT."**

Table 1. *Timetable 1998, e-mails, facsimiles, and actions. *Quotations ("italics") are exact texts from e-mails.*

3.3.2 Task 2: Analysis of shear-wave splitting measurements

We had hoped to use several additional stations in the shear-wave window at SAU to investigate why observed time-delays between split shear-waves in Iceland are approximately twice those usually observed elsewhere, and why time delay values show large scattering. Unfortunately, financial constraints prevented installation of additional SIL stations.

The range of time-delays between split shear-waves is found to vary between different regions worldwide and sometimes between different stations in the same region. Time-delays vary with crack density, crack aspect ratio, and isotropic P- and S-wave velocities. These effects can be calculated, and are reasonably well understood. Time-delays are also observed to be higher in regions with high heat flow (Crampin 1994) and this is believed to be the main reason for the larger values observed in Iceland. Also following the increase in Band-1 time-delays before the Vatnajökull eruption in 1996, the level of time-delays has been decreasing for both Band-1 and Band-2 by approximately 2 ms/km over 1997-1998. It would appear that the crust has been slowly adjusting to the strain released by the eruption as the mid-Atlantic ridge gradually takes up the change in strain.

However, the large scatter of time-delays and polarizations is difficult to explain. During the last two big earthquakes (November 1998 near BJA and June 2000 near SAU) it was observed that the scatter in time-delays increases considerably with the onset of the earthquake and the large scatter continues for several weeks thereafter (Figures 10a and 10b). It is hoped that the controlled source SMSITES project will help to resolve this difficulty.

3.3.3 Task 3: Establish shear-wave splitting map of Iceland

Figure 9 shows a map with roundels and equal-area rose diagrams of shear-wave splitting polarizations at stations with more than about ten arrivals within the shear-wave window out to 45°. Experience suggests that an overall shear-wave splitting map is not particularly useful as was first thought. Optimum procedures seem to require individual studies of shear-wave splitting at individual stations.

3.3.4 Task 4: Calibrate techniques and behaviour if and when changes are identified

Stress-forecasting using small earthquakes as the source of shear-waves is only possible when there is a more-or-less continuous source of small earthquakes. As we have seen, this is extremely rare. To stress-forecast earthquakes without such persistent activity, requires cross-well seismology using a borehole source transmitting orthogonally polarized shear-waves along appropriate ray paths in Band-1 to three-component borehole receivers in further boreholes.

These boreholes exist in northern Iceland near Húsavík close to the Flatey-Húsavík fault of the Tjörnes fracture zone, and an EU project (*SMSITES: Developing stress-monitoring sites and infrastructure for forecasting earthquakes,* contract no. EVR1-CT1999-4000) developing a Stress-Monitoring Site (SMS) has recently started. The SW of Iceland has proved to be a very active seismic area during the last years. However, shear-wave splitting analysis near the Húsavík transform fault and Grímsey zone has not been very productive up to now, due to lack of continuous swarm activity in the shear-wave windows of the northern stations, GRI, SIG, LEI, and others. The new technique of controlled source measurements are expected to monitor changes in shear-wave splitting near Húsavík more efficiently, as well as reduce the scattering in the time-delays.

3.3.5 Task 5: Incorporate shear-wave splitting interpretations into routine analysis

The only successful technique yet established for automatically identifying polarization directions and time-delays from digital records of shear-wave splitting is the Cross-Correlation Function, or CCF technique of Gao et al. (1998). CCF was used on SIL records from SW-Iceland. It was not successful (Volti and Crampin 2000). The reason is thought to be that the data that was used to test CCF was an isolated swarm of small earthquakes, whereas the foci in Iceland are more distributed so that shear-waves propagate along significantly different ray paths. This suggests that reliable automatic reading of shear-wave splitting in Iceland is unlikely to be successful.

3.3.6 Meetings and conferences

PRENLAB contractor meetings:
Stuart Crampin and Theodora Volti: The second PRENLAB-2 workshop, Húsavík, Iceland, July 30, 1998.
Theodora Volti: The fifth PRENLAB-2 workshop, Nice, France, April 27, 2000.

Presentations of PRENLAB results:
Stuart Crampin: 60th annual EAGE meeting, Leipzig, Germany, June 8-12, 1998.
Stuart Crampin: Tenth biennal EUG meeting, Strasbourg, France, March 28 - April 1, 1999.
Stuart Crampin: 61th annual EAGE meeting, Helsinki, Finland, June 7-11, 1999.
Stuart Crampin: The second EU-Japan workshop on seismic risk, Reykjavík, Iceland, June 23-27, 1999.
Stuart Crampin: XXII IUGG General Assembly, Birmingham, United Kingdom, July 18-30, 1999.
Stuart Crampin: 9th International Workshop on Seismic Anisotropy, Houston, Texas, USA, March 26-31, 2000.
Stuart Crampin: 62nd annual EAGE meeting, Glasgow, United Kingdom, June 25-30, 2000.
Stuart Crampin: 70th annual SEG meeting, Calgary, Alberta, Canada, August 6-11, 2000.

3.3.7 References

Crampin, S. 1994. The fracture criticality of crustal rocks. *Geophys. J. Int.* 118, 428-438.

Crampin, S. 1999. Calculable fluid-rock interactions. *J. Geol. Soc.* 156, 501-514.

Gao, Y., P. Wang, S. Zheng, M. Wang & Y.-T. Chen 1998. Temporal changes in shear-wave splitting at an isolated swarm of small earthquakes in 1992 near Dongfang, Hainan Island, Southern China. *Geophys. J. Int.* 135, 102-112.

Volti, T. & S. Crampin 2000. Shear-wave splitting in Iceland: four years monitoring stress changes before earthquakes and volcanic eruptions. *Geophys. J. Int.*, submitted.

3.4 Subproject 4: Borehole monitoring of fluid-rock interaction

Contractor:

Frank Roth
Section: Earthquakes and Volcanism
Division: Solid Earth Physics and Disaster Research
GeoForschungsZentrum Potsdam (GFZ)
Telegrafenberg
D–14473 Potsdam
Germany
Tel: +49–331–288–1210
Fax: +49–331–288–1203
E–mail: roth@gfz-potsdam.de

Subcontractor:

Valgarður Stefánsson
National Energy Authority (Orkustofnun, OS)
Grensásvegur 9
IS–108 Reykjavík
Iceland
Tel: +354–569–6004
Fax: +354–568–8896
E–mail: vs@os.is

3.4.1 Geophysical logging

In the preparatory phase of an earthquake, stress accumulation is expected to be connected with the creation of borehole breakouts (BOs), changes in the number and size of cracks, a possible variation of the stress direction, etc. Therefore it is very important to monitor the following set of geoparameters:

- P–wave travel time.
- electrical conductivity.
- stress information from borehole breakouts (orientation and size).
- crack density.

In the framework of this project, we had the chance to carry out repeated logging to obtain a time series of logs in the South Iceland seismic zone (SISZ). An 1100 m deep borehole (LL–03, Nefsholt) inside the zone (63.92°N, 20.41°W, 7 km south of the seismic station SAU) was used and provided the unique opportunity to perform measurements much nearer to earthquake sources than usual – the hypocenter depths at that location range between 6 and 9 km. Moreover, data could be obtained for a depth interval of more than 1000 m, uninfluenced by the sedimentary cover and less disturbed by surface noise.

This was achieved by repeated logging with tools as: sonic log (BCS), gamma-ray (GR), spectral gamma-ray (SGR), neutron-neutron log, dual induction/latero log (DIL), 16"- and 64"-normal resistivity log, spontaneous potential log (SP), a borehole temperature log (BHT), four-arm-dipmeter (FED), and borehole-televiewer (BHTV).

The neutron-neutron log, the 16"- and 64"-resistivity log, the SP log, and temperature logs were run with the logging equipment of OS, the rest with the Halliburton logging truck of GFZ.

Investigations on the stress field in the SISZ

Besides the repetition of logs in borehole LL–03 (Nefsholt), we performed single logging campaigns at other boreholes to check the state of the regional stress field. This is important for two reasons:

- From the San Andreas fault we know (Zoback et al. 1987) that fault zones may be in a low stress state between earthquakes, which gets visible through stress orientations perpendicular and not pointing at an angle of 30° to 45° to the strike-slip fault. To determine the present state of stress in the SISZ, it is important to see if there are stress components, that are not perpendicular to existing faults and thus favour earthquakes on them.

- The SISZ is no typical transform zone. Looking at the orientation of rift opening and the adjacent rifts, one would expect a left–lateral strike-slip zone in NW-SE direction (N103°E) to connect the Reykjanes ridge and the eastern volcanic zone (EVZ) of Iceland. Instead earthquakes occur on en–echelon N–S striking right–lateral faults. Assuming an angle of 45° between the maximum horizontal compressive stress and the fault (as it is done constructing fault plane solutions) both planes are equivalent. However, from a rock mechanics point of view, expecting an angle of about 30° between fault and maximum horizontal principal stress, the stress orientation at N-S striking faults should be N30°E, compared to N60°E at an E-W striking transform.

3.4.2 Task 1: Repeated logging in borehole Nefsholt

All together 7 logging campaigns took place. The locations are shown in Figure 11. Table 2 lists the logs performed during the project.

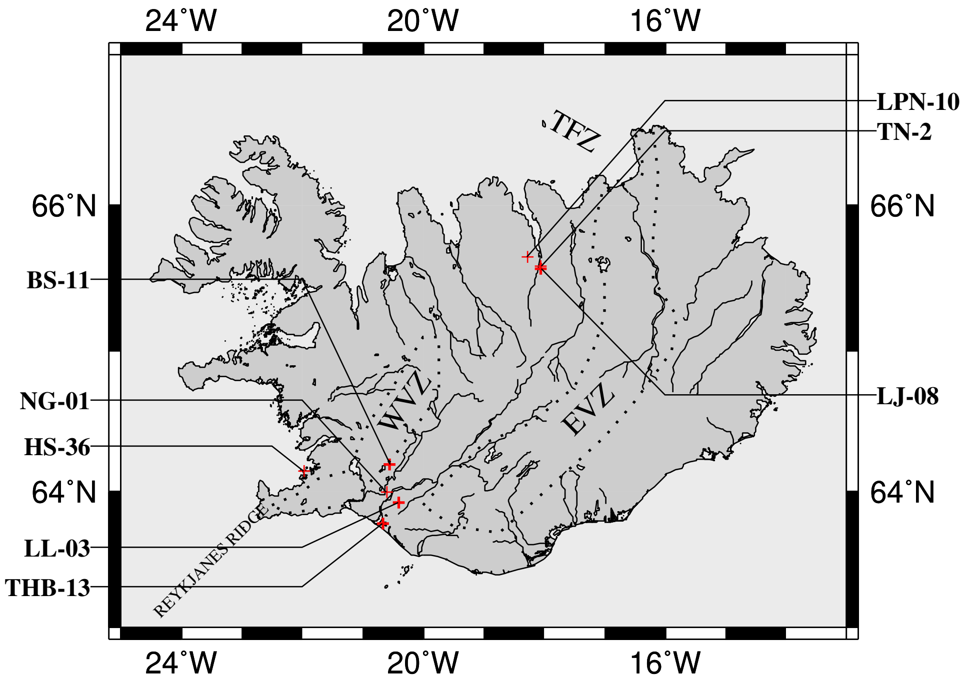

Figure 11. *Map of Iceland showing the location of the site of repeated logging (LL-03) and of the other boreholes, where measurements have been performed. The SISZ extends between the southern ends of the WVZ and EVZ. Wells LL-03 and NG-01 are inside the SISZ, BS-11 is north, THB-13 is south of the zone.*

Altogether, the seven campaigns have contributed to the two aims of this Subproject, that are:

- Observation of changes in physical parameters of the rock, in the degree of fracturing, and in the orientation of principal stresses with respect to seismic activity.
- Indirect measurement of tectonic stress orientation to evaluate the tectonic stress field in the area of the SISZ. For that, the borehole geometry was observed for certain structures, that allow to determinate the orientation of the horizontal principal stress, as there are borehole breakouts and vertical tensile fractures. Borehole breakouts are failures of material of the borehole wall, that result from accumulation of tangential

stress at the borehole wall at the azimuth of the lower horizontal principle stress (σ_h), caused by the free surface produced by drilling. In a linear elastic isotropic theory, this would be perpendicular to the maximum horizontal principal stress (σ_H). Alternatively, at this free surface, the tensile strength of the borehole wall can be exceeded at the azimuth of the maximum principal horizontal stress, what produces vertical fractures along σ_H. These vertical fractures extend in the direction of the maximum and open in the direction of the minimum horizontal principal stress. The occurrence of these tensile fractures can be enhanced by thermal stress caused by cold water pumped into the well.

Orkustofnun provided a lithology log of the well LL-03 at Nefsholt. This log is based on cuttings (rock pieces crushed while drilling), not on cores, what strongly limits its depth resolution. It shows a nearly continuous sequence of altered basalt, interrupted only by a few thin sedimentary layers and some thin layers of dolerite, hyaloclastites and fresh basalt. Different kind of layers show different characteristic sets of logs, that allow to distinguish between the lava flows and the sediments (Figure 12, Table 4). The result, i.e. the correlation with the rock physical parameters, is very reasonable: The sedimentary layers seem to contain more water (larger pore space) entailing higher travel times of elastic waves, lower resistivity and higher absorption of neutrons. The correlation is an important indicator that the log results have good quality.

Name:	Location:	Max. depth:	Logged interval:	Tools used:	Date:
NG–01	Ólafsvellir (inside SISZ)	1070 m	180–1070 m	FED, GR	July 1996
HS–36	Reykjavík	980 m	330–980 m	BHTV, BCS-GR	July 1996
LPN-10	Laugaland near Akureyri, North Iceland	890 m	80–880 m	BHTV, BCS-DIL-GR	July 1996
LJ–08	Syðra–Laugaland near Akureyri	2740 m	120–1890 m 120–1330 m 500–1980 m	FED, BHTV, BCS-DIL-GR, BHTV	July 1996 June 1998
TN–02	Ytri-Tjarnir near Akureyri	1370 m	260–1370 m	BCS, GR	July 1996
LL–03	Nefsholt (inside SISZ, site of repeated logging)	1309 m	80–1100 m	BHTV, BCS-DIL-GR SGR BHT neutron–neutron X-Y–caliper 16"- and 64"- resistivity SP	July 1996 October 1996 September 1997 December 1997 June 1998 September 1997 June 1998 April 1999 August 2000 April 1999 October 1999 September 1996 April 1999 October 1999 August 2000 October 1999
THB–13	Þykkvibær SW of Hella near the south coast	1254 m	466–1225 m	BHTV	December 1997
BS–11	Böðmóðsstaðir near Laugarvatn, north of the SISZ	1193 m	703–1090 m 500–1090 m	BHTV	December 1997 June 1998

Table 2. *All logs performed during both PRENLAB projects. As borehole NG-01 partly collapsed between log runs, the hole was abandoned and well LL-03 was chosen for repeated logging. GR indicates gamma-ray log, SP stands for spontaneous potential, 16" for short normal resistivity tool, and 64" for long normal resistivity tool. FED means four-arm-dipmeter, which includes an oriented four-arm-caliper. BHTV and BHT mean ultrasonic borehole televiewer and borehole temperature, respectively. BCS is borehole compensated sonic log; DIL is dual induction/latero log. The deepest parts of wells LJ-08, LL-03, THB-13, and BS-11 were not accessible anymore.*

Log type:	Date:	Depth range:	File name:	Remarks:
Temperature log (T)	07-07-1977	0–920	T07071977	
Temperature log	18-10-1977	0–1100	T18101977	
Temperature log	17-09-1980	0–1060	T17091980	
Temperature log	25-06-1992	0–1106	T25061992	
Temperature log	23-04-1999	4–1080	21415	
Temperature log	03-08-2000	0–1087	T03082000	
Natural gamma log (GR)	23-04-1999	0–1080	21424	
Natural gamma log	27-10-1999	10–1080	22588	
Neutron-neutron log (NN)	23-04-1999	3–1080	21421	
Neutron-neutron log	27-10-1999	10–1080	22585	+
Neutron-neutron log	03-08-2000	7–1087	N03082000	
Self potential log (SP)	27-10-1999	25–1080	22570	
16" normal resistivity log (SN)	27-10-1999	25–1080	22568	*
16" normal resistivity log	03-08-2000	27–1087	S03082000	*
64" normal resistivity log (LN)	27-10-1999	25–1080	22569	*
64" normal resistivity log	03-08-2000	27–1087	L03082000	*
LL3 of DIL	07-1996	36–1070	LL3-07/96	
LL3 of DIL	12-1997	37–1071	LL3-12/97	

Table 3. *Repeated logging by Orkustofnun in Well LL-03, files used for comparisons. + : depth adjusted to neutron-neutron log of August 2000. * : calibrated and depth adjusted to neutron-neutron log of August 2000.*

Depth interval:	GR:	BCS travel time:	neutron–neutron water content porosity:	DIL, 16", 64" resistivity:	Lithology:
265-275 m	low	low	low	high	altered basalt
275-280 m	low	high	high	low	sediment
280-285 m	low	low	low	high	altered basalt
285-298 m	high	high	high	low	sediment
298-305 m	high	low	low	high	fresh basalt

Table 4. *Characteristic set of log values for different kinds of layers, derived from Figure 12.*

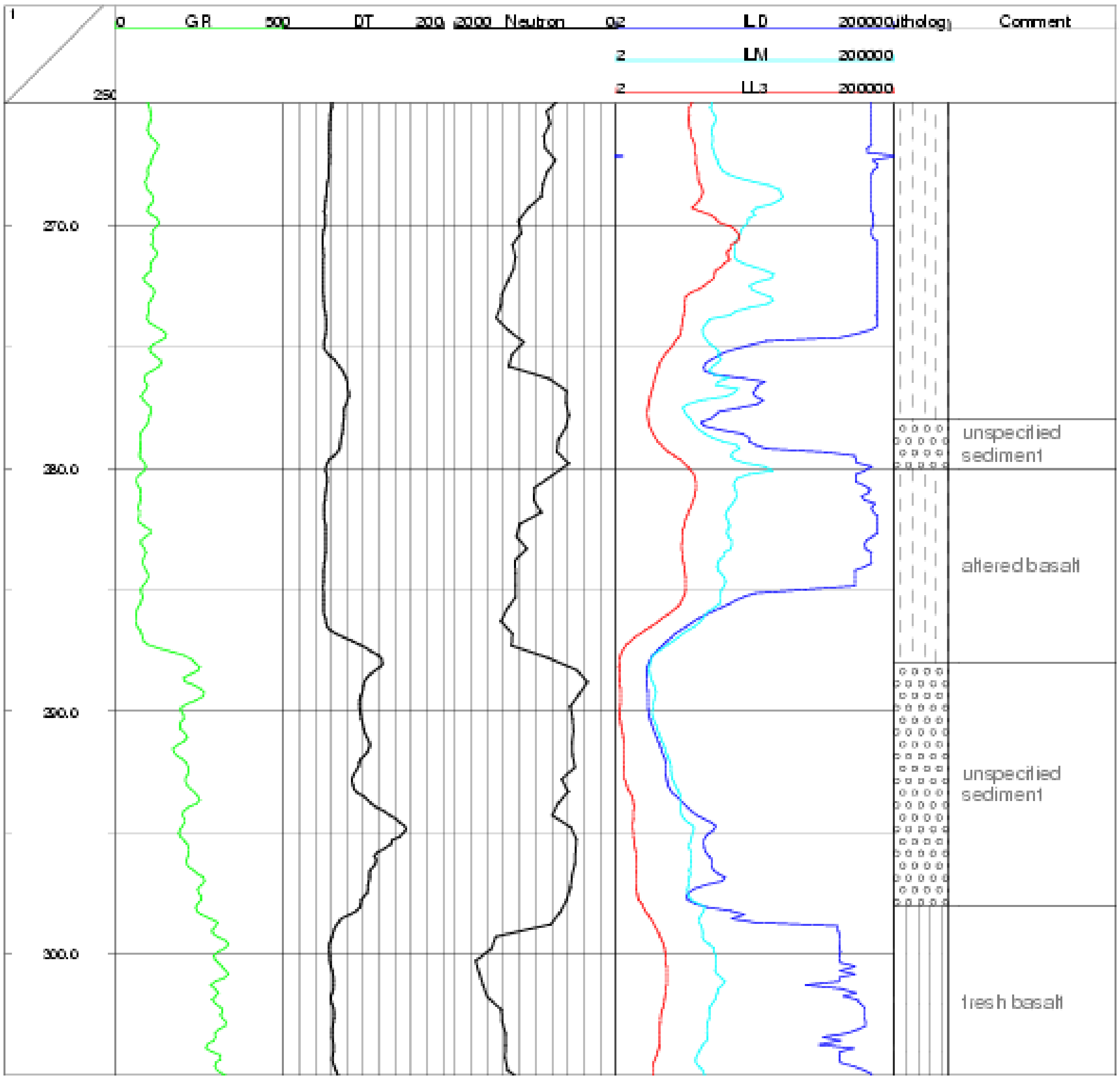

Figure 12. *Data example showing the correlation between the performed logs and the lithology based on the analysis of cuttings provided by Orkustofnun. GR = gamma–ray in API units, DT = compensated travel time in microseconds per foot, Neutron = neutron–neutron log in API units, ILD = induction log of deep penetration in* Ωm*, ILM = induction log of medium penetration in* Ωm*, and LL3 = latero log in* Ωm*.*

3.4.3 Tasks 2, 3, and 4: Cross correlation of logs of the same type from different campaigns and earlier loggings; comparison of changes in logs of different type; comparison of changes in logs with changes in seismicity, etc.

Due to a delay in the year 2000 logging campaign, we had the chance to take at least some data after the two June 2000 earthquakes in the SISZ. Comparing the data of July 1996 to October 1999 with those of August 2000 gives the opportunity to see which parameters have changed across the time from before the event to 6 weeks after.

And there were remarkable changes at the borehole. Our coworker Steinar Þór Guðlaugsson reports: "Water started to flow from well LL-03 on July 20–22 after a rapid rise in the water table from a depth of several meters since the earthquakes. This was probably caused by changes in crustal stress resulting from the earthquakes, although reinjection into the Laugaland geothermal field, which was initiated recently, may also have played some role. On August 3, the flow-rate was 0.5 l/s." The effects seen in the logs will be described below.

Repeated logs in LL–03: borehole temperature

The longest time series of logs is available in the temperature logs (BHT). There are data from the time of the drilling of the well (1977), later from 1980 and 1992, and finally from 1999 and 2000 taken during the work in the PRENLAB projects. The temperature logs are plotted together in Figures 13 and 14. Following a heating phase after drilling, the temperatures went down. The most recent of the logs predating the earthquakes show a regime of inflow into the well at several feed-points and downward flow of this fluid to a depth of 830 m where it re-enters the formation. The new log of August 2000 can be interpreted in two different ways: (1) The fracture at 830 m now feeds water into the well in addition to the other feed-points and above this depth water everywhere flows upwards; (2) Water now flows upwards above the feed-point at 120 m, whereas below this depth water continues to flow down the well to a depth of 830 m as before. In either case, it is evident that water entering the well at feed-points in the 200-250 m depth range is warmer than before. Temperature differences between the feed-points in this depth range also seem to have increased. At present it is unclear whether this is caused by changes in the fracture network feeding this interval or by the reinjection.

In conclusion, a comparison of the August 2000 temperature log with the earlier ones does not reveal any new water-conducting fractures (feed-points), but does show changes in the temperature and flow rate of the water flowing through previously existing fractures. These changes may probably be explained by a combination of stress change (general increase in formation pressure) associated with the earthquakes and reinjection, but do not rule out movements on some of the fractures feeding the well.

Repeated logs in LL–03: latero log and "normal" resistivity tools, self potential
The latero log (the one included in the GFZ DIL tool is of LL3 type) and the "short normal" resistivity tool of OS (16" electrode spacing) are designed for shallow penetration into the formations. Whereas the "induction log medium" and "induction log deep" of the DIL tool and the "long normal" resistivity tool (64") are dedicated for investigations deeper into the rock surrounding the borehole.

The latero log resistivity shows good repeatability (see red curves in Figure 15). So do the 16" and 64" tools, as will be discussed later. Figure 16 gives a comparison of LL3 logs from 2 different campaigns with logs of the short and long normal resistivity tools. The LL3 curves correlate very well besides a small depth shift. They also correlate qualitatively well with the other two logs, but there seems to be a calibration problem in the LL3, leading to much lower values than the other tools. We did not care about this, as only changes in the logs were of interest here. The match between the normal resistivity tools is expected to be moderate as their penetration depths are different. There was no indication of changes in LL3 logs before June 2000.

The resistivity logs from before and after the June 2000 events are plotted together in Figure 17. Two kinds of adjustments were made to the final logs before they were plotted: Firstly, a correction was applied to the logs based on a calibration carried out at the surface with a set of known resistances. Secondly, the origin of the August 2000 neutron-neutron log was taken as a common depth reference and the logs shifted to this datum.

The new logs agree remarkably well with those obtained in 1999. The main change observed is a decrease in the 16" resistivity log above 110 m. This can probably be explained by the increased temperature (and – less likely – salinity) in this depth range caused by the newly established upflow. Too much should not be read from the differences between the 16" logs in the 400-700 Ohmm range, because of the large correction that was applied to the 1999 log as a result of the surface calibration. The differences may simply reflect the inaccuracy of the correction. Keeping this in mind, the only significant difference between the 16" resistivity logs that may require other explanations seems to be a decrease in resistivity in the 465-470 m depth interval.

The main change in the 64" resistivity log is a decrease in resistivity from 150-155 m. This may or may not be associated with the upflow. We also note a slight decrease in the 465-470 m range which correlates spatially with the main anomaly in the 16" log. At the same depth, the spontaneous self potential log (SP) of October 1999 shows an anomaly too (cf. Figure 18), which could indicate a crack, existing already at that time (there is no SP log of August 2000). A possible interpretation of the 3 correlating signals might be a crack that has widened but does not feed-in water with a temperature different from the local temperature in the borehole.

The long normal tool shows variations between October 1999 and August 2000 also at depths other than 465 m and at resistivities lower than 400 Ohmm. They usually display lower values in August 2000, which could mean that water filled cracks have opened. However, none of the variations is also seen in the "short normal" log, which leads to doubts on real changes in rock physical parameters, as new cracks could be formed much more easily near the borehole wall, an area sampled by the 16" tool. See also the discussion on the neutron-neutron log.

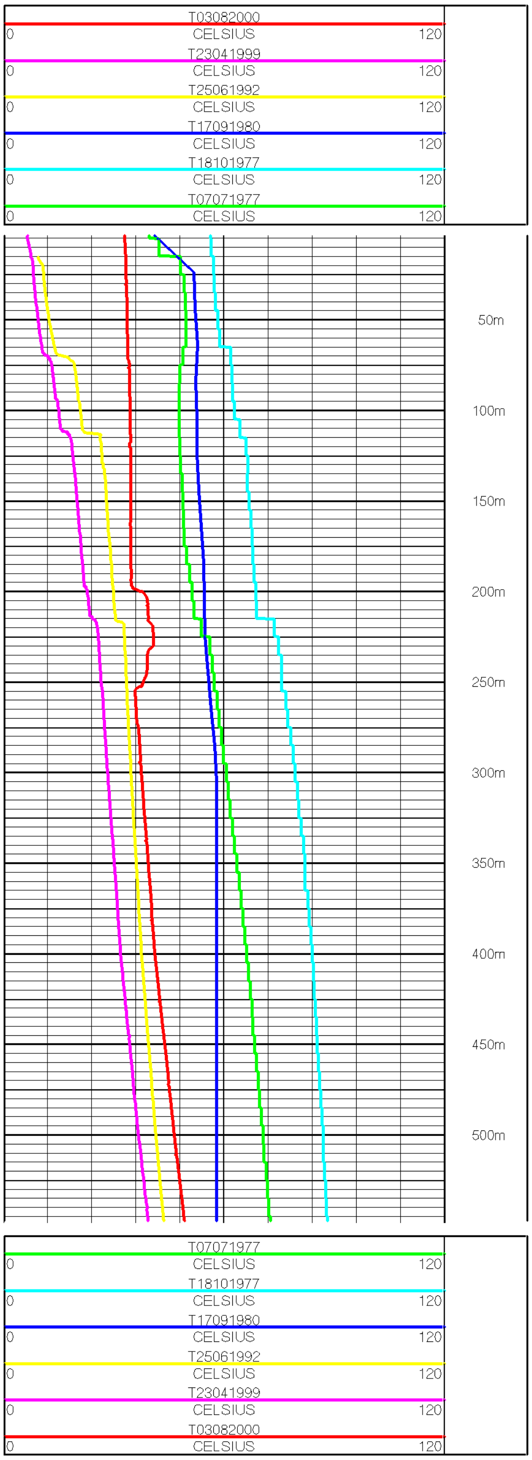

Figure 13. *Borehole temperature logs since the drilling of well LL-03. Numbers following "T" give date of log.*

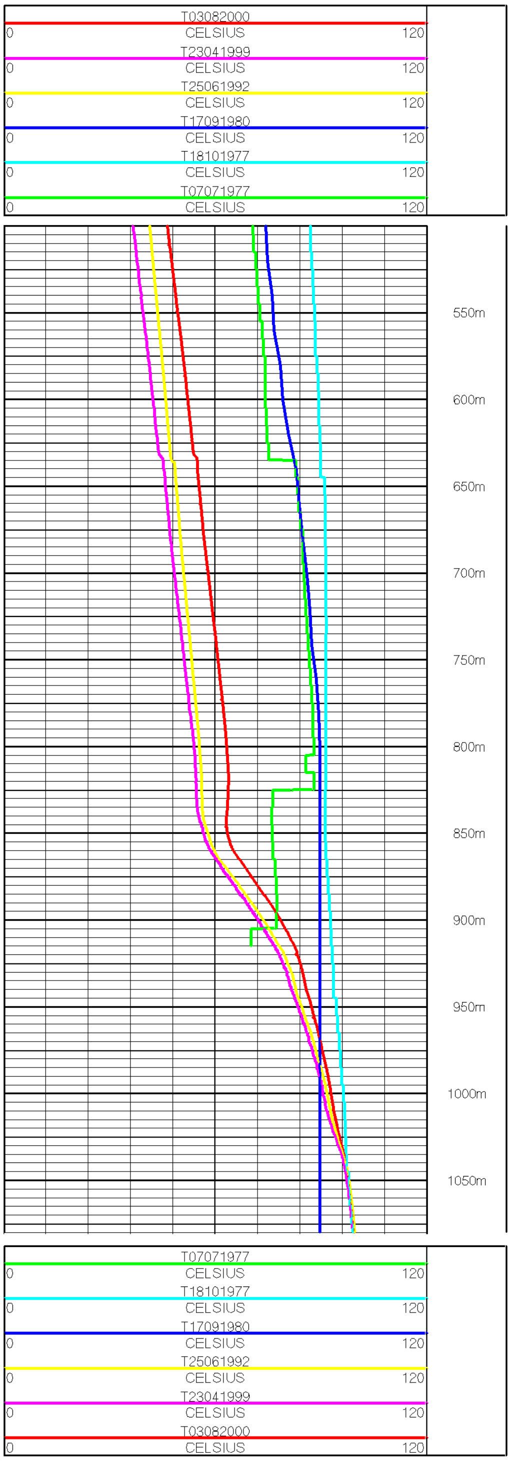

Figure 14. *Borehole temperature logs since the drilling of well LL-03. Numbers following "T" give date of log.*

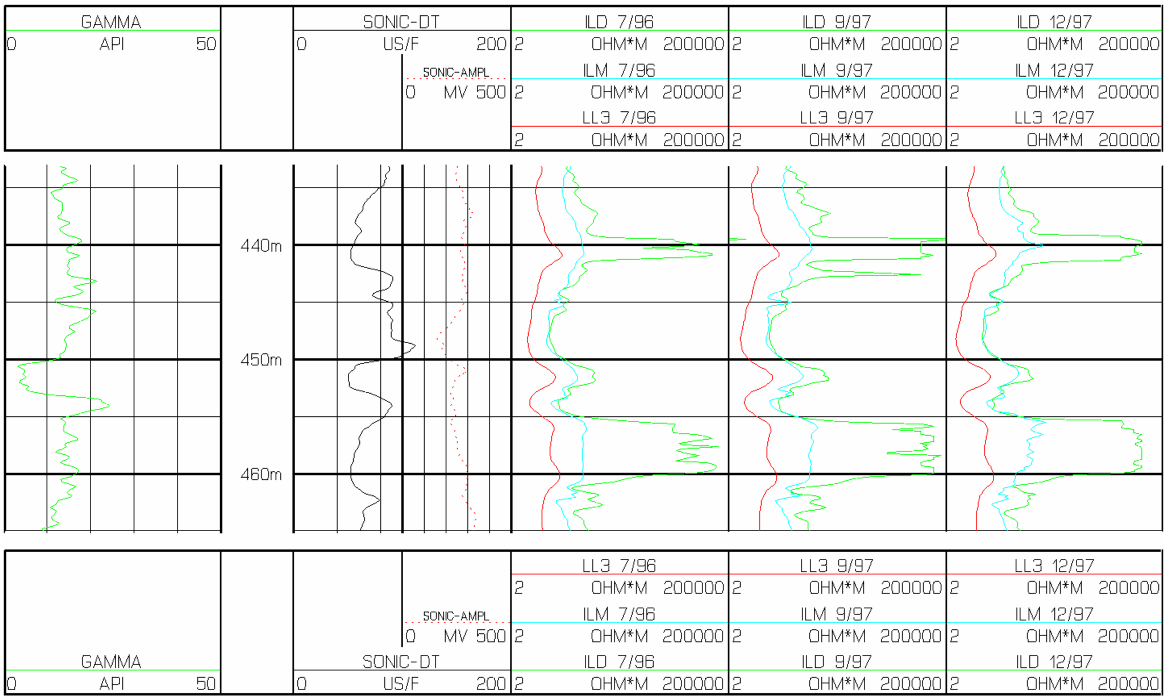

Figure 15. *Data example showing from left to right: gamma–ray log in API units, compensated travel time in microseconds per foot and the sonic amplitude, and three repeated measurements of latero log (LL3), induction log of medium penetration (ILM) and induction log of deep penetration (ILD). Month and year of campaign are given.*

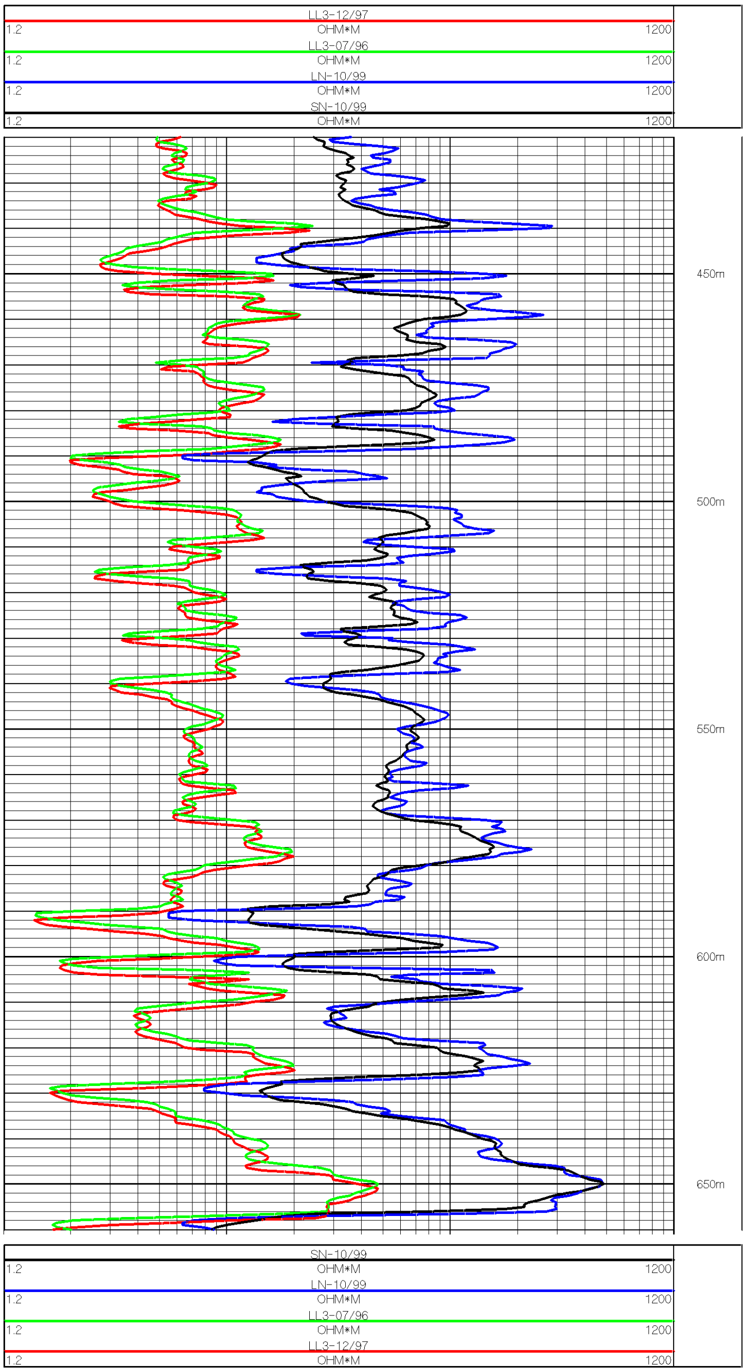

Figure 16. *Data example showing latero log data (LL3) from July 1996 and December 1997 together with short (SN) and long normal (LN) resistivity data from October 1999.*

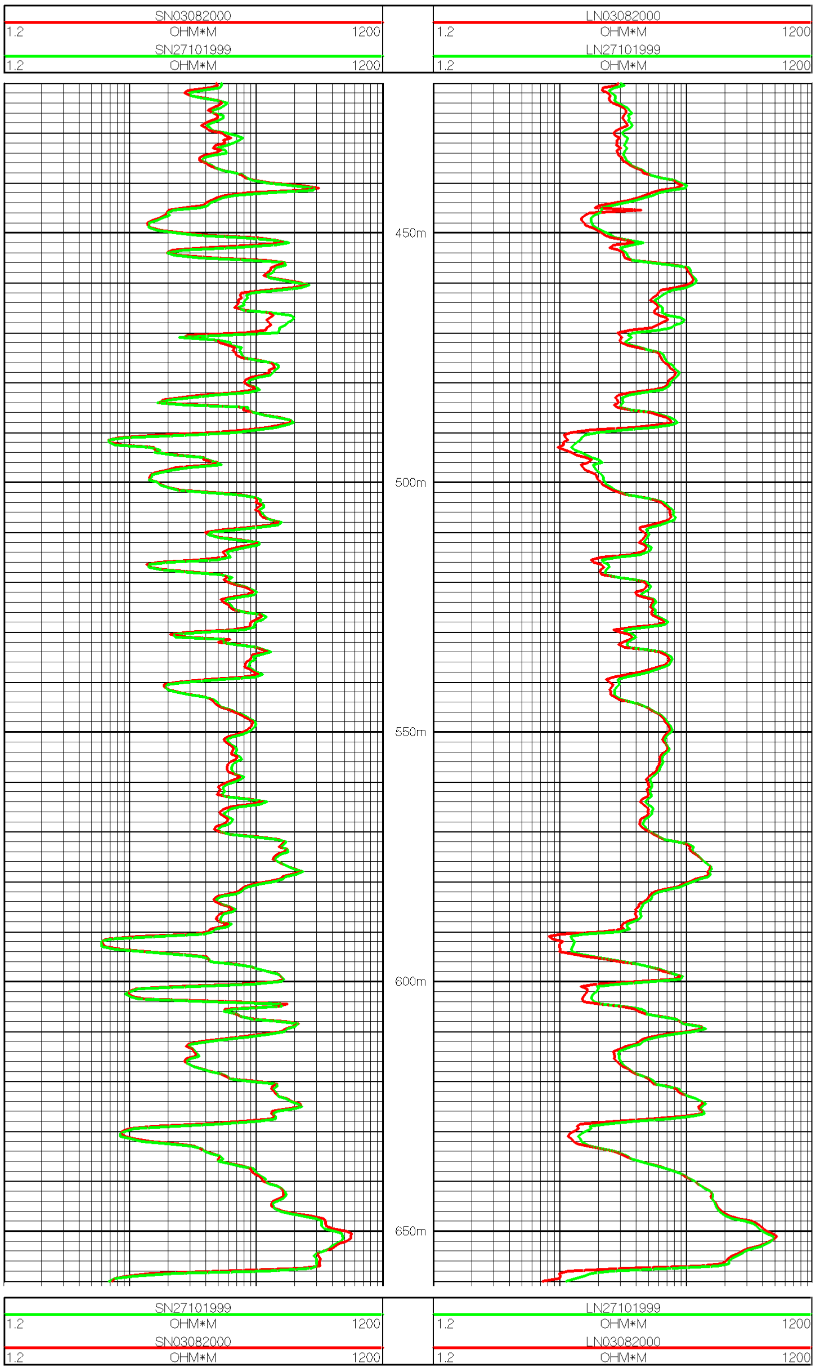

Figure 17. *Data example comparing short (SN) and long normal (LN) resistivity data from October 1999 and August 2000.*

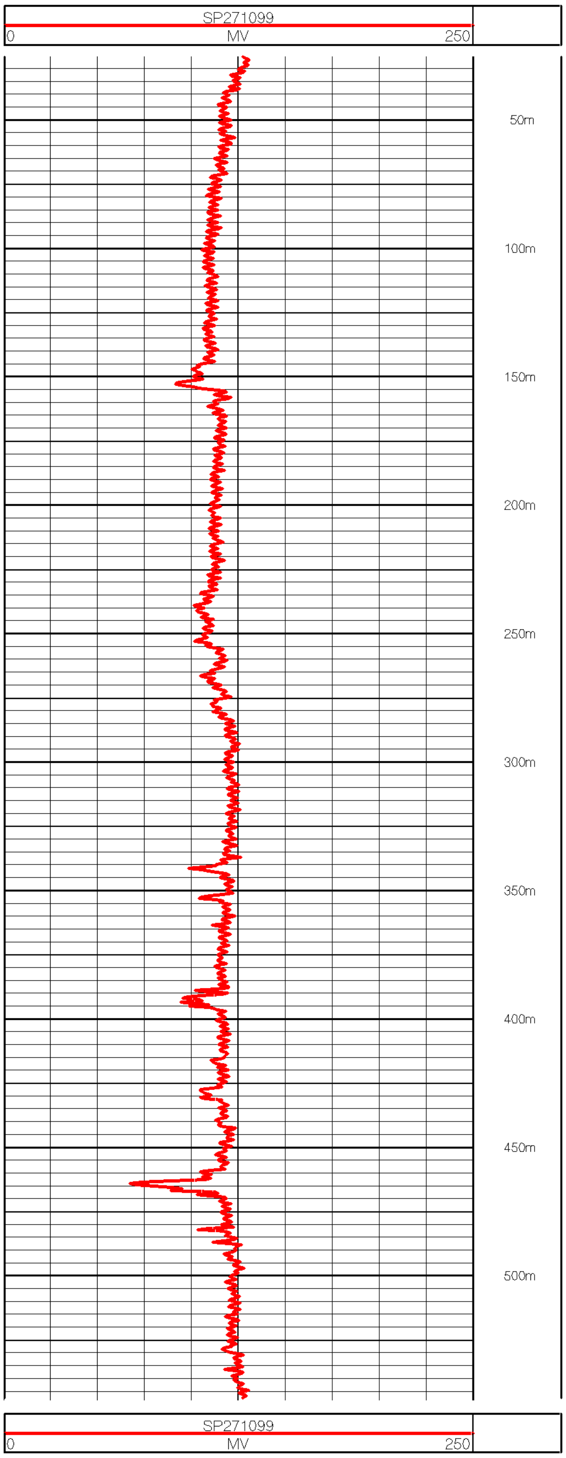

Figure 18. *Data example comparing short (SN) and long normal (LN) resistivity data from October 1999 and August 2000.*